Magnetic properties of Fe-rich amorphous Fe-La alloys

1990 J. Phys.: Condens. Matter 2 417

(http://iopscience.iop.org/0953-8984/2/2/017)

J. Phys.: Condens. Matter **2** (1990) 417–429. Printed in the UK

Magnetic properties of Fe-rich amorphous Fe–La alloys

H Wakabayashi, T Goto, K Fukamichi† and H Komatsu†
Institute for Solid State Physics, University of Tokyo, Roppongi, Minato-ku, Tokyo 106, Japan
† Department of Materials Science, Faculty of Engineering, Tohoku University, Sendai 980, Japan

Received 2 May 1989, in final form 3 August 1989

Abstract. A magnetic phase diagram of Fe-rich amorphous $Fe_{100-x}La_x$ alloys has been determined from high-field magnetisation and AC susceptibility measurements. The alloys with $x > 10$ are ferromagnetic, but show a re-entrant spin glass behaviour at low temperatures. The ferromagnetic state becomes unstable when x approaches 10. For $x \leqslant 10$, the ferromagnetic state disappears and a direct transition from a paramagnetic to a spin glass state is observed. Extrapolation of the phase diagram to $x = 0$ suggests that pure amorphous Fe is no longer a ferromagnet but a spin glass with a freezing temperature of about 110 K. The irreversible process of magnetisation characterising the theoretically proposed spin glass picture has been observed in the low-temperature phases of the alloys.

1. Introduction

Recent investigations on amorphous (a-) Fe-based binary alloys indicate that the ferromagnetism becomes unstable when they are highly concentrated with Fe. Fe-rich a-$Fe_{100-x}G_x$ (G = metalloid) alloys such as a-$Fe_{100-x}B_x$ exhibit a normal ferromagnetic (FM) behaviour with relatively high Curie temperatures (e.g. $T_C > 450$ K for a-$Fe_{100-x}B_x$ with $x > 10$) (Fukamichi *et al* 1979, Chien and Unruh 1982), but both the Curie temperature and the average magnetisation per Fe atom deduced from the saturation magnetisation measurements decrease as x approaches zero (Hiroyoshi *et al* 1978). Among a-$Fe_{100-x}(ET)_x$ (ET = early transition metal), a-$Fe_{100-x}Zr_x$ has been investigated most extensively. It is ferromagnetic for $x \leqslant 55$ (Unruh and Chien 1983). The Curie temperature increases to a maximum value at $x \sim 20$ and decreases rapidly as x decreases. At low temperatures the alloy shows a spin-glass-like behaviour, for example, the thermomagnetic history, the asymmetric hysteresis loop (Hiroyoshi and Fukamichi 1981, 1982) and the large high-field susceptibility (Hiroyoshi *et al* 1983). Saito *et al* (1986) concluded from the AC susceptibility measurements that a-$Fe_{92.4}Zr_{7.6}$ is near the critical concentration below which the ferromagnetic order collapses, and that alloys with $x < 7.6$ may show the direct transition from a paramagnetic (PM) to a spin glass (SG) phase. A similar conclusion was attained later by Ryan *et al* (1987a). Some authors rejected the spin glass picture and attributed the unusual low-temperature behaviour to an exponential increase of magnetic hardness in a normal ferromagnet due to domain wall pinning by antiferromagnetic inclusions (Read *et al* 1984, 1986). a-$Fe_{100-x}Hf_x$ shows a similar behaviour to a-$Fe_{100-x}Zr_x$ (Hiroyoshi *et al* 1985, Ryan *et al* 1987b). Quite

0953-8984/90/020417 + 13 $03.50

contrary to these alloy systems, a-$Fe_{100-x}Y_x$ alloys do not have a ferromagnetic phase, but show a SG transition in the composition range $x < 60$ (Coey *et al* 1981, Chappert *et al* 1981). The SG temperature increases with decreasing x and is saturated to be about 110 K for $x < 20$.

All the results described above suggest that the instability of ferromagnetism occurs in highly concentrated Fe-based amorphous alloys (Fukamichi *et al* 1989). Present investigations on Fe-rich a-$Fe_{100-x}La_x$ is intended to achieve a better understanding of the ferromagnetic instability and the magnetic properties of pure amorphous Fe. We chose La as a glass former for the following reasons: (i) among ET elements, La has the largest glass-forming ability as it has the largest atomic radius and the largest electronegativity difference against Fe, and the amorphous state can thereby be stabilised with the smallest amount of glass former (Fukamichi and Hiroyoshi 1985); (ii) the Fe–La alloy system forms no intermetallic compound (Kubaschewski 1982), which ensures that the alloy is in the amorphous state from chemical short-range ordering corresponding to a crystalline phase; (iii) there has not been much work done on the system (Heiman and Kazama 1979, Kazama *et al* 1980) and no results have been obtained for the Fe-rich region $x < 15$.

2. Experimental procedure

Bulk a-$Fe_{100-x}La_x$ alloys 0.1–0.3 mm thick with nominal compositions x of 7.5, 10.0, 12.5, 15.0, 17.5, 20.0, 25.0, 30.0, 35.0, 40.0, 45.0 and 50 were prepared by high-rate DC sputtering at an Ar gas pressure of 40 mTorr and a target voltage of 1.0 kV. They were deposited onto water-cooled Cu substrates of 45 mm diameter and were confirmed to be amorphous by x-ray diffraction. The substrates were dissolved away in a solvent of $H_2O(1000\,cm^3) + CrO_3(500\,g) + H_2SO_4(27\,cm^3)$. Strip samples (typically $1.5 \times 12 \times 0.2\,mm^3$) were used for the magnetic measurements where external fields are applied along the longest axes.

The magnetisation curves up to 90 kOe were measured by an extraction-type magnetometer with a superconducting magnet. The high-field magnetisation measurements up to 240 kOe were made by an induction method with a wire wound pulse magnet. Duration time of the pulse field was 9 ms. The AC susceptibility measurements were performed by means of a conventional mutual inductance technique at a frequency of 80 Hz in a field amplitude of 1 Oe. The non-linear AC susceptibility was measured simultaneously for a-$Fe_{92.5}La_{7.5}$ by detecting the third higher harmonic of the induced signal.

3. Results and discussion

3.1. Magnetic phase diagram of the Fe-rich a-$Fe_{100-x}La_x$

We first present the overall magnetic properties of Fe-rich a-$Fe_{100-x}La_x$. The magnetisation curves at 4.2 K up to 90 kOe are shown in figure 1. The magnetisation with $x \geqslant 20$ is almost saturated at 40 kOe as for a normal ferromagnetic, but the saturation is incomplete for $x < 20$ even at 90 kOe.

We extended the magnetisation measurements at 4.2 K for a-$Fe_{82.5}La_{17.5}$ and a-$Fe_{92.5}La_{7.5}$ up to 240 kOe using a pulse magnet. The results are shown in figure 2. The

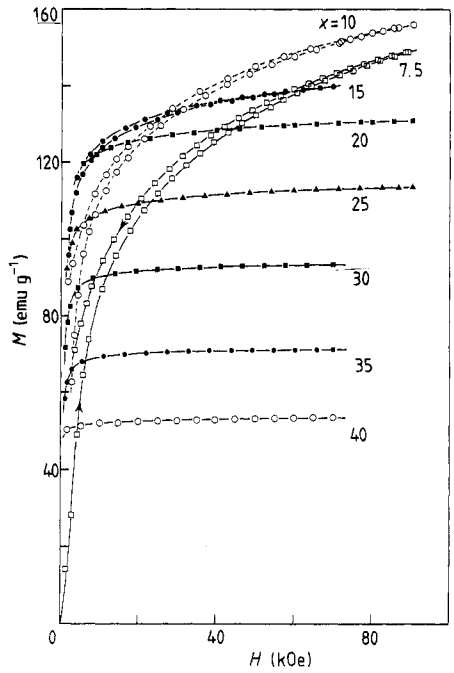

Figure 1. High-field magnetisation (M) curves of a-$Fe_{100-x}La_x$ at 4.2 K in steady fields (H) up to 90 kOe.

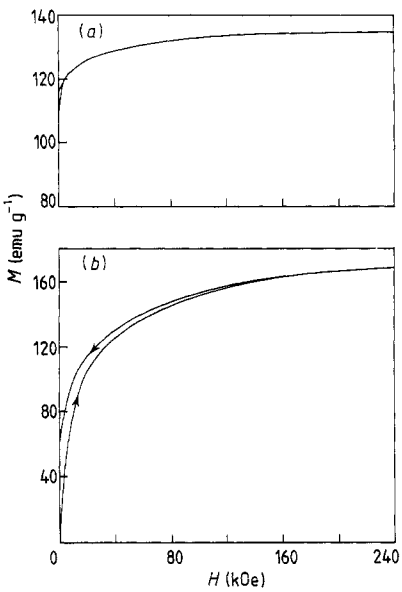

Figure 2. High-field magnetisation (M) curves of (a) a-$Fe_{82.5}La_{17.5}$ and (b) a-$Fe_{92.5}La_{7.5}$, both at 4.2 K in pulsed fields (H) up to 240 kOe.

magnetisation of a-$Fe_{82.5}La_{17.5}$ is completely saturated above 140 kOe. For a-$Fe_{92.5}La_{7.5}$, anomalously large hysteresis is observed up to about 150 kOe, but the saturation is almost achieved at the maximum field of 240 kOe. The anomalously large saturation fields imply that a non-collinear spin structure is realised in both samples. Since random

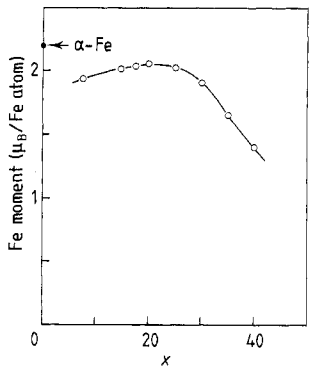

Figure 3. Saturation magnetisation of a-$Fe_{100-x}La_x$ determined from the high-field magnetisation curve.

local anisotropy of single-ion type cannot be a dominant mechanism hampering parallel alignment of spins to the applied field in such amorphous alloys without non-S state 4f elements, the non-collinear spin structure must be caused by the existence of antiferromagnetic interactions.

We determined the saturation magnetisation of a-$Fe_{100-x}La_x$ by extrapolating the data in the saturation region linearly to zero field. The results are plotted in figure 3. With increasing x, the saturation value increases up to 2.06 μ_B/Fe at $x = 25$ and then decreases slightly in the lower concentration region. The results are consistent with those of the Mössbauer measurements, which has been reported elsewhere (Wakabayashi *et al* 1989).

The temperature dependence of the AC susceptibility for a-$Fe_{100-x}La_x$ is shown in figure 4. As the temperature decreases, the AC susceptibility increases for $x = 25$–35 sharply at the Curie temperature (T_C) to a maximum value, keeps almost constant and then drops off abruptly at low temperatures. This behaviour is typical of a re-entrant spin glass (RSG) or a mictomagnet. The drop-off of the susceptibility is usually related to the transition from a FM to a RSG state (Verbeek *et al* 1978). Since the onset of the drop-off is rather vague, the transition temperature (T_f) is defined by the 'shoulder' in the temperature dependence of the susceptibility. As for the samples with $x = 12.5$–20 and 40–50, the PM–FM transition is somewhat smeared. The AC susceptibility begins to increase gradually just above T_C. These results are in contrast with earlier work (Heiman and Kazama 1979, Kazama *et al* 1980), which characterises a-$Fe_{100-x}La_x$ with $x = 17.5$–31 as a simple ferromagnet. They could not observe the RSG behaviour because they measured the magnetisation only in static fields above 1 kOe. The AC susceptibility with $x \leqslant 10$ does not show any sharp increase corresponding to the PM–FM transition, but exhibits a cusp characterising a direct PM–SG transition at a temperature of T_g. Thus no FM phase persists in this concentration range. This observation is quite consistent with the results of the magnetisation measurements described above.

Three kinds of transition temperatures T_C, T_f and T_g are plotted on the magnetic phase diagram of a-$Fe_{100-x}La_x$ shown in figure 5. The Curie temperature rises to a maximum value of 289 K at $x = 30$ and then falls rapidly for $x < 15$ with decreasing x. This behaviour has been observed in common in ferromagnetic Fe-rich amorphous alloys as described in the Introduction. The development of antiferromagnetic interactions must be responsible for the decrease of the Curie temperature because there is no abrupt decrease in the average Fe moment as shown in figure 3. This development is also verified by the fact that the magnetic saturation becomes extremely difficult in the

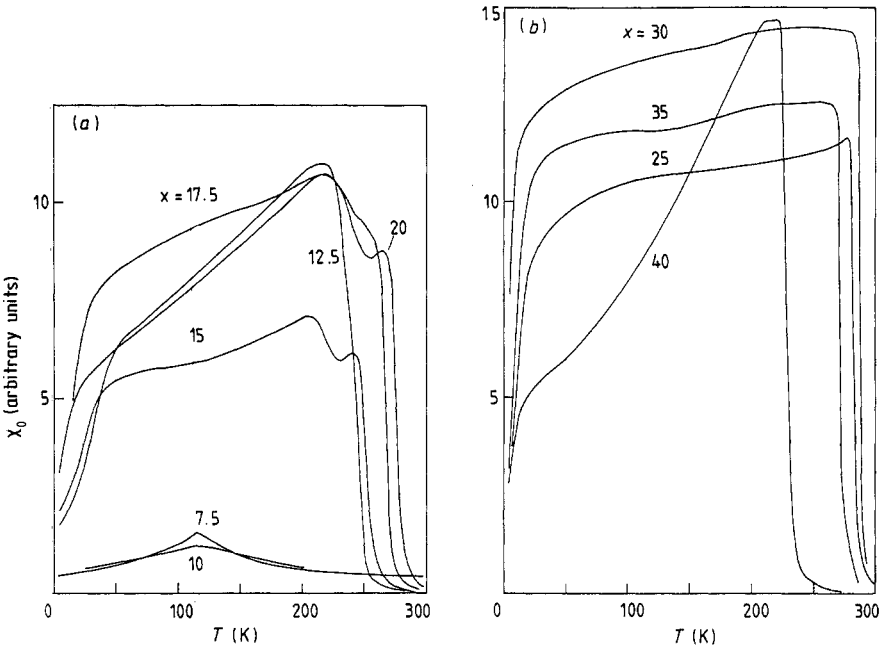

Figure 4. Temperature dependence of the AC susceptibility χ_0 for a-$Fe_{100-x}La_x$: (*a*) $7.5 \leqslant x \leqslant 20$; (*b*) $25 \leqslant x \leqslant 40$.

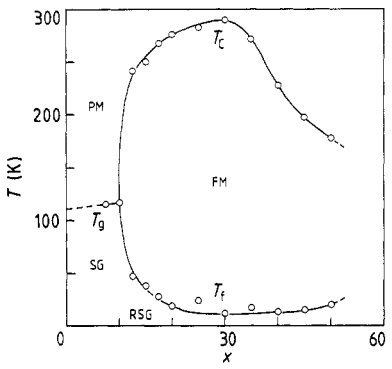

Figure 5. Magnetic phase diagram of a-$Fe_{100-x}La_x$ determined from the temperature dependence of the AC susceptibility.

concentration range $x < 15$ (see figure 1). The magnetic phase diagram indicates that the three lines of T_C, T_g and T_f meet at $x = 10$–11.

3.2. Magnetic properties of the most Fe-concentrated a-$Fe_{100-x}La_x$

In this section, we discuss the SG behaviour of a-$Fe_{100-x}La_x$ with $x \leqslant 10$ using the results of a-$Fe_{92.5}La_{7.5}$. The temperature dependence of the magnetisation in several constant fields is shown in figure 6. Both the zero-field-cooled magnetisation (M_{ZFC}) and the field-cooled one (M_{FC}) were measured on heating after the sample was cooled from room temperature to 4.2 K. The two measurement curves for $H > 50$ Oe merge into one curve

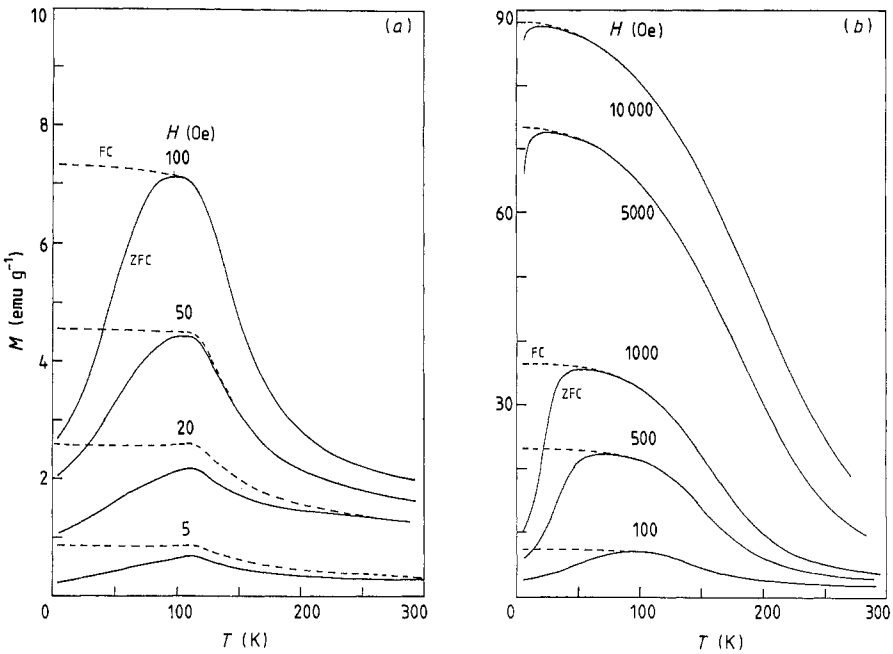

Figure 6. Temperature dependence of the zero-field-cooled and field-cooled magnetisation for a-$Fe_{92.5}La_{7.5}$ in various magnetic fields: (*a*) $H \leq 100$ Oe, (*b*) $100 \leq H \leq 10000$ Oe.

at T_g and the magnetisation is reversible above T_g as in normal SG systems. However, the magnetisation measured at 5 Oe is irreversible up to room temperature. The value of M/H corresponding to the susceptibility depends on the field even at temperatures well above T_g and the temperature dependence does not obey the Curie–Weiss law at any value of H. These results suggest that the high-temperature phase above T_g is not simply paramagnetic. The non-linear response to the field and the deviation from the Curie–Weiss law above T_g are reminiscent of the development of short-range ferromagnetic order or the formation of ferromagnetic clusters. We distinguish the concept of ferromagnetic short-range order from that of the ferromagnetic cluster as follows: the former describes the small region where spins are ferromagnetically correlated, but fluctuate with time. The time average of magnetisation in this region is zero in zero applied field. On the other hand, the latter means a much larger region containing a large enough number of spins to maintain a thermodynamically stable ferromagnetic state within the region. Since the irreversible behaviour persists up to 280 K, the short-range-order picture cannot explain the field cooling effect. On the other hand, M_{FC} must be different from M_{ZFC} if some ferromagnetic clusters are formed: the magnetisation in each cluster takes a direction parallel to the local easy axis of the cluster if the cluster is formed in zero applied field, whereas the magnetisation may have a larger component parallel to the field direction if the cluster is formed in the applied field. The fact that a comparatively small field of about 50 Oe can suppress the irreversible behaviour suggests that the field can align the ferromagnetic clusters formed in zero applied field. The number of clusters is considered to be very small because they cannot be detected by the Mössbauer experiment (Wakabayashi *et al* 1989).

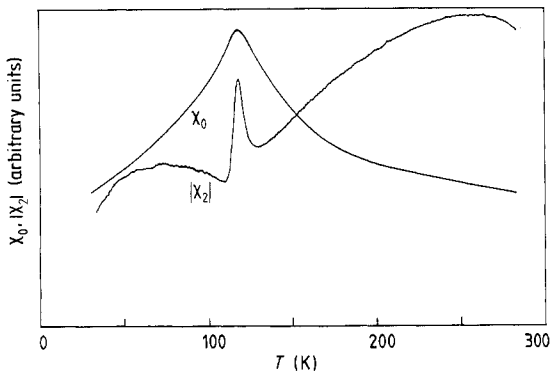

Figure 7. Temperature dependence of the non-linear AC susceptibility χ_2 for a-$Fe_{92.5}La_{7.5}$. The AC susceptibility χ_0 is also shown for comparison.

Figure 7 displays the non-linear AC susceptibility (χ_2) as well as the AC susceptibility (χ_0) for a-$Fe_{92.5}La_{7.5}$ measured simultaneously in an AC field of 10 Oe at 80 Hz. In addition to the sharp anomaly centred at T_g, two broad peaks at around 70 and 250 K are found in the temperature variation of χ_2, whereas χ_0 shows no anomaly on both sides of the cusp at T_g. It should be noted that the sign of χ_2 is negative which is opposite to the sign of χ_0. The peak of χ_2 at T_g is so steep that it is regarded as the divergence of χ_2, which is well established theoretically as well as experimentally in spin glass systems (Chowdhury 1986). The fact that the centre peak of χ_2 is found only in the vicinity of T_g suggests that the transition at T_g is a cooperative phase transition rather than a blocking of some magnetic entities. On the contrary, the other two peaks of χ_2, situated on either side of the central one, are very broad, indicating that any uniform phase transition does not take place. Considering the results of the magnetisation measurements, the most likely situation is that some ferromagnetic clusters are formed successively above T_g as the temperature is lowered. Such magnetically inhomogeneous behaviour must result from the fluctuation of exchange interactions, which in turn results from the concentration fluctuation. Referring to the magnetic phase diagram of figure 5, a more Fe-concentrated region than average composition is not ferromagnetic and cannot be responsible for the broad peak of χ_2 above T_g. On the other hand, a less Fe-concentrated region (10–15 at.% La) is ferromagnetic with the Curie temperature less than 260 K, which is in accordance with the peak around 250 K. The lower temperature peak around 70 K is more difficult to assign. One possibility is that this broad peak corresponds to the RSG transition of the above ferromagnetic clusters.

3.3. Magnetic properties of less Fe concentrated a-$Fe_{100-x}La_x$

The Fe-rich a-$Fe_{100-x}La_x$ with $x > 10$ is ferromagnetic but indicates the RSG behaviour at low temperatures as described in § 3.1. The Curie temperature becomes a maximum at $x = 30$. As x deviates from 30, the Curie temperature decreases and the PM–FM transition is somewhat smeared.

Figure 8 shows the ZFC magnetisation M_{ZFC} and the FC magnetisation M_{FC} for a-$Fe_{82.5}La_{17.5}$ in several applied fields. In fields higher than 50 Oe, an irreversibility appears well below $T_c = 265$ K, while a weak irreversibility persists up to a much higher temperature (240 K) near T_C at $H = 20$ Oe. This behaviour is observed for $x = 12.5$–20 and $x = 40$–50. On the other hand, the weak irreversibility in the low field is not found for

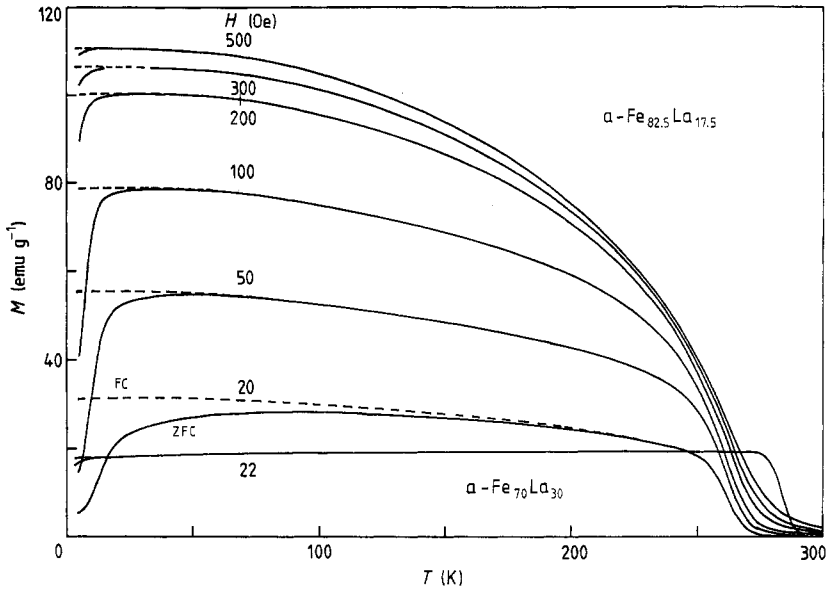

Figure 8. Temperature dependence of the zero-field-cooled and field-cooled magnetisation for a-$Fe_{82.5}La_{17.5}$ in various magnetic fields. For comparison, the experimental data of a-$Fe_{70}La_{30}$ in a field of 22 Oe are also shown.

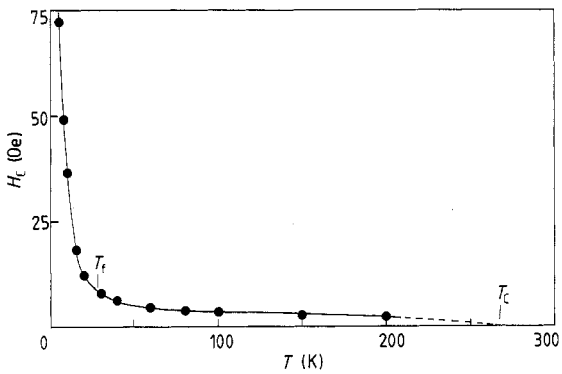

Figure 9. Temperature dependence of the coercive force for a-$Fe_{82.5}La_{17.5}$.

x = 25–35. The ZFC and FC magnetisation of a-$Fe_{70}La_{30}$ at 22 Oe is shown for comparison in figure 8. The PM–FM transition is not smeared, but is well defined by a sharp increase of the magnetisation up to the demagnetisation limit. The irreversibility of the magnetisation appears only at low temperatures, well below T_C.

Apart from the weak irreversibility, the strong irreversible behaviour of the magnetisation observed well below T_C as well as the drop-off of the AC susceptibility for $x > 10$ are usually regarded as evidence of the RSG behaviour. However, some investigators (Read *et al* 1984, 1986) attributed these behaviours to a low-temperature increase of magnetic hardness in a normal ferromagnet. Indeed the coercive force of a-$Fe_{82.5}La_{17.5}$ increases drastically near the RSG temperature determined by the AC susceptibility measurements as shown in figure 9.

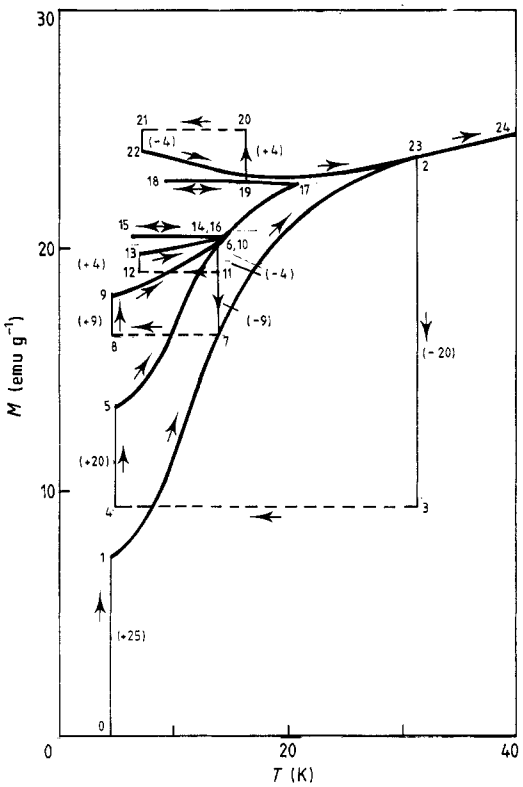

Figure 10. Irreversible magnetisation process of a-$Fe_{82.5}La_{17.5}$ in the RSG phase. The measurement procedure is described in detail in the text.

To elucidate this point, we examined the magnetisation process of a-$Fe_{82.5}La_{17.5}$ in detail, as shown in figure 10. The measurement was made in the order of the numbers on the figure. The bold curves indicate the temperature sweep process in the constant field $H_0 = 25$ Oe. The lines represent the magnetisation change due to the field change ΔH at a constant temperature. The field change ΔH (in Oe) is shown in parentheses. The broken line indicates the temperature sweep process in the field $H_0 + \Delta H$. After zero-field cooling to the point 0, the magnetisation measurement starts in the field H_0 from the point 1. If the system is heated without changing the field, the magnetisation traces the curve $1 \rightarrow 24$, which indicates the usual temperature variation of M_{ZFC}. If the field is reduced by $-\Delta H$ at a certain halfway temperature T_2, the magnetisation decreases ($2 \rightarrow 3$). This process is reversible. After the field cooling in the reduced field $H_0 - \Delta H$ ($3 \rightarrow 4$) to a lower temperature T_4, an increase of the field by the same amount ΔH at T_4 puts the system in a different state with a different magnetisation ($4 \rightarrow 5$) from the state where the system originally started at the same temperature and field (T_4, H_0). Thus the subsequent heating in the field H_0 produces a different curve (branch) on the M–T diagram. The interesting fact is that this new curve retraces back to the original curve at T_2 where the field was reduced at the beginning ($5 \rightarrow 2$). Furthermore, we can draw similar cycles from an arbitrary point on this new branch with different field changes ($6 \rightarrow 7 \rightarrow 8 \rightarrow 9 \rightarrow 10$, $10 \rightarrow 11$ . . .), producing an arbitrary number of branches. The heating process after cooling from any point without changing the field, which is the special case of the above cycles, is reversible ($14 \rightarrow 15 \rightarrow 16$, $17 \rightarrow 18 \rightarrow 19$). If the field is increased by ΔH from H_0 at any temperature, the irreversibility in the magnetisation

appears (19 → 20). The subsequent field cooling in $H_0 + \Delta H$ and field reduction by $-\Delta H$ at a lower temperature also produces a new state (20 → 21 → 22). However, the magnetisation in the temperature sweep in H_0 does not return back to the point 19 where the field was originally changed, but retraces back to the original curve at a much higher temperature (22 → 23): the cycle does not close in this case. Thus all the states produced by the cooling in the temporally reduced field are governed by the state at the temperature where the field is changed, and even the states produced by the cooling in the temporally increased field are governed by a past state at a higher temperature.

The irreversible behaviour described here is naturally interpreted by the theoretically proposed picture of the SG phase where a large number of metastable states corresponding to minima (valleys) of the free energy exist in the phase space (e.g. Palmer 1983). The states with different magnetisations at the same temperature T and field H_0 (represented by the bold curves in figure 10) may correspond to states in the different valleys branched from a single valley at a higher temperature T' by the field cooling in the temporally reduced field. Here we suppose that the field reduction by $-\Delta H$ followed by the field increase by ΔH at a constant temperature does not produce irreversibility: this procedure does not put the system on a different valley, which is consistent with the experimental results. On the other hand, the field increase before the field reduction at T puts the system in a different valley, producing some irreversibility, but this valley is considered to be branched from a valley at a higher temperature $T' > T$. The low-temperature increase of the coercive force shown in figure 9 is attributed to the enormous increase in the number of valleys at low temperatures.

The SG picture, however, is not always applied to the interpretation of the irreversible behaviour of magnetisation because a ferromagnetic character is not lost even at the lowest temperature, and thereby the change of magnetisation must reflect the domain wall motion in some way. However, it is very difficult to explain the above behaviour in terms of simple thermal activation of the domain wall motion. For example, there is no reason for the magnetisation at the point 5 or 22 in figure 10 to return back to the point 23, if the magnetisation at the point 1 changes to the point 5 or 22 by overcoming a large number of energy barriers produced by the usual wall-pinning mechanism. The following three facts are also favourable to the SG picture: (*a*) the same irreversible behaviour has also been found in a-$Fe_{92.5}La_{7.5}$ without the FM phase; (*b*) all the features of this irreversible behaviour of the magnetisation have been reproduced by a simplified mean-field numerical approach to the Ising system (Soukoulis *et al* 1983), in which competing nearest-neighbour interactions are randomly distributed on a two-dimensional square lattice (30 × 30) with a zero-mean Gaussian distribution (Wakabayashi 1988); (*c*) our recent Mössbauer study on a-$Fe_{82.5}La_{17.5}$ has found that an anomalous increase in the average hyperfine field sets in at 70 K above T_f (Wakabayashi *et al* 1989). Since the increase of hyperfine field is ascribed to a random freezing of the transverse component of spins perpendicular to the FM ordering (Takeda *et al* 1985), the RSG phase can be characterised as a mixed phase with the FM and the SG ordering. Thus, domain formation due to the existence of FM ordering as well as the magnetisation process must be affected by the freezing of the transverse component. We believe that the unusual irreversible behaviour observed in $Fe_{82.5}La_{17.5}$ is quite different from that in a simple ferromagnet and has spin glass character.

It is expected that the alloys with more than 50% La lose the FM phase and show a PM–SG transition near the onset of ferromagnetism. The nature of this SG phase and its origin are probably different from that of highly Fe-concentrated alloys, but they are outside the scope of this paper.

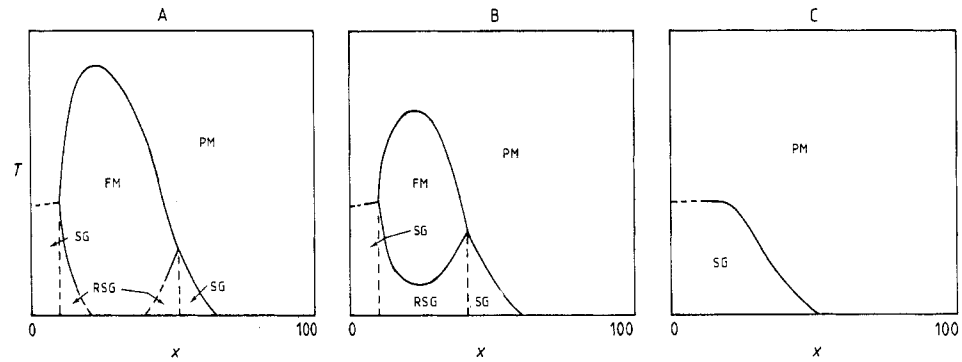

Figure 11. Three types of schematic phase diagrams, A, B and C, realised in the a-$Fe_{100-x}ET_x$ alloy systems. The A type is observed in a-Fe–Zr and a-Fe–Hf, the B type in a-Fe–La, a-Fe–Ce and a-Fe–Lu, and the C type in a-Fe–Y.

3.4. Magnetism of pure amorphous Fe

In order to discuss magnetism of pure amorphous Fe, schematic phase diagrams observed in the a-$Fe_{100-x}ET_x$ alloy systems are shown in figure 11. They can be classified into three types (Fukamichi *et al* 1989). The A type phase diagram consists of the following six concentration regions indicating different magnetic properties: (*a*) PM → SG, (*b*) PM → FM → RSG, (*c*) PM → FM, (*d*) PM → FM → RSG, (*e*) PM → SG and (*f*) PM, which appear successively as the concentration x increases. In a-Fe–Zr and a-Fe–Hf systems (Hiroyoshi *et al* 1985, Saito *et al* 1986, Ryan *et al* 1987a, b), (*a*) has not been observed clearly in the Fe-rich region yet, but their phase diagrams are considered to be essentially A type. The B type does not have (*c*), where the FM phase region is usually narrower than that in the A type. The phase diagram of a-Fe–La belongs to the B type. Our recent studies on a-Fe–Ce and a-Fe–Lu systems (Fukamichi *et al* 1988, Goto *et al* 1990) revealed that their phase diagrams are A type. The C type does not have (*b*), (*c*) and (*d*) because an FM phase disappears. This unique phase diagram was discovered in the a-Fe–Y system (Coey *et al* 1981, Chappert *et al* 1981). In the a-Fe–G alloy systems, on the other hand, (*a*) and (*b*) seem to be absent in the Fe-rich region (Fukamichi *et al* 1979, Chien and Unruh 1982). Xiao and Chien (1987) found that simple extrapolation of the Mössbauer parameters such as hyperfine fields, centre shift and quadruple splitting to pure amorphous Fe for various a-Fe–ET systems are different from those for the a-Fe–G systems. They suggested that the structural short-range order in a-Fe–ET is quite different from that in a-Fe–G. Since chemical bonding between Fe and G atoms strongly affects not only the structural short-range order in a-Fe–G but also the magnetic properties (Fujiwara 1984), a-Fe–G systems are not suitable for estimating the magnetic properties of pure amorphous Fe.

As described above, the a-Fe–ET alloys show SG behaviour in very high Fe concentration ranges. Because T_g of a-$Fe_{92.5}La_{7.5}$ is slightly lower than that of a-$Fe_{90}La_{10}$ (115 K and 117 K, respectively), T_g is expected to have a weak concentration dependence. The extrapolation of T_g suggests that pure amorphous Fe shows a PM–SG transition at about 110 K. This is consistent with the A type phase diagram of a-Fe–Y (Coey *et al* 1981) and the B type phase diagrams of a-Fe–Zr (Saito *et al* 1986, 1989), a-Fe–Ce (Fukamichi *et al* 1988) and a-Fe–Lu (Goto *et al* 1990). The extrapolation made by Ryan

et al (1987a) gives a rather higher value of $T_g = 150$ K. This value, however, seems to be less convincing because their most Fe-concentrated a-Fe–Zr alloy is still ferromagnetic and the actual PM–SG transition has not been observed yet.

The existence of SG and RSG states in the Fe-rich a-Fe–ET alloys at low temperatures indicates that the alloys are random spin systems with competing ferromagnetic and antiferromagnetic interactions. The origin of antiferromagnetic interactions is often ascribed to an FCC-like coordination of Fe atoms and shorter Fe–Fe bonds (Forester *et al* 1979). The instability of FM order and the FM to AF phase transition observed in the relevant crystalline compound $La(Fe_xAl_{1-x})_{13}$ with increasing x are considered to be due to an increase in the number of Fe nearest neighbours and a decrease in the lattice parameters (Palstra *et al* 1985). Our recent AC susceptibility measurements at high pressures on a-$Fe_{87.5}La_{12.5}$ revealed that a pressure of 20 kbar can completely wash out the susceptibility increase at T_C, and produce a typical SG cusp at around 110 K (Goto *et al* 1989). This fact clearly shows that short Fe–Fe interatomic spacing is responsible for the development of antiferromagnetic interactions and the appearance of the SG phase. According to the x-ray structure analysis of a-$Fe_{100-x}La_x$, however, significant change is not found in the average nearest-neighbour Fe–Fe interatomic distance for $x = 10$–15 (Matsuura *et al* 1989). The increase in the nearest-neighbour Fe–Fe coordination number is considered to be more important to the instability of the FM state in a-$Fe_{100-x}La_x$ from a structural point of view.

Kakehashi (1987) showed using a finite-temperature theory for itinerant-electron systems that a new type of itinerant-electron SG appears in FCC Fe alloys such as Fe–Ni, where antiferromagnetic interactions originate from local environment effects through a strong non-linear coupling between Fe atoms with magnetic moments less than 1.7 μ_B surrounded by more than ten Fe nearest neighbours. The antiferromagnetic interactions in the Fe-rich amorphous alloys are considered to be derived from the same origin as in the FCC Fe–Ni alloys. The extension of the above theoretical approach to the non-crystalline system is very important for understanding the magnetism of Fe-rich amorphous alloys.

4. Conclusions

The evolution of magnetic order is clearly observed in the Fe-rich a-$Fe_{100-x}La_x$ alloys as the concentration approaches pure Fe. The significant difficulty of the magnetic saturation at 4.2 K and the lack of rapid increase of the AC susceptibility indicate that ferromagnetism is not retained in the alloys with $x \leqslant 10$. The SG phase of the alloys is well characterised by the AC susceptibility cusp with the divergent peak of non-linear susceptibility. Because there is no sign of the reduction of the average Fe magnetic moment in this concentration region, the SG system is unique in the sense that the SG phase is observed in the magnetically concentrated metallic system with a single kind of magnetic element. The less Fe-concentrated alloys become ferromagnetic, but show the RSG transition at low temperatures. The RSG behaviour of the alloys is very similar to that observed in other a-Fe–ET alloys, but the existence of the RSG phase is more evident in the present alloys because ferromagnetism is actually lost in the highest Fe concentration region. The magnetic phase diagram obtained suggests that pure amorphous Fe is no longer a ferromagnet but a spin glass with a transition temperature of about 110 K. This conclusion is consistent with the magnetic phase diagrams of various Fe-rich amorphous Fe–ET alloys.

Acknowledgments

We are indebted to Professor A Ito, Professor M Matsuura and Dr S Morimoto for numerous suggestions and stimulating discussions. We are also grateful to Dr T Sakakibara and Mr S Todo for assistance in the magnetisation measurements.

References

Chappert J, Coey J M D, Lienard A and Rebouillat J P 1981 *J. Phys. F: Met. Phys.* **11** 2727–44
Chien C L and Unruh K M 1982 *Phys. Rev.* B **25** 5790–6
Chowdhury D 1986 *Spin Glasses and Other Frustrated Systems* (Singapore: World Scientific) pp 121–5, 295–300
Coey J M D, Givord D, Lienard A and Rebouillat J P 1981 *J. Phys. F: Met. Phys.* **11** 2707–25
Forester D W, Koon N C, Schelleng J H and Rhyne J J 1979 *J. Appl. Phys.* **49** 7336–41
Fujiwara T 1984 *J. Non-Cryst. Solids* **61–62** 1039–41
Fukamichi K, Komatsu H, Goto T and Wakabayashi H 1989 *MRS Int. Mtg. Advanced Materials* vol 11 ed M Homma and Y Imakoa (Pittsburgh, PA: Materials Research Society) p 285–99
Fukamichi K and Hiroyoshi H 1985 *Sci. Rep. RITU* A **32** 154–66
Fukamichi K, Komatsu H, Goto T and Wakabayashi H 1988 *Physica* B **149** 276–80
Fukamichi K, Masumoto T and Kikuchi M 1979 *IEEE Trans. Magn.* **MAG-15** 1404–9
Goto T, Murayama C, Mori N, Wakabayashi H, Fukamichi K and Komatsu H 1989 *J. Physique Coll.* **49** C8 1143–4
Goto T *et al* 1990 *J. Phys. Soc. Japan* to be published
Heiman N and Kazama N 1979 *Phys. Rev.* B **19** 1623–32
Hiroyoshi H and Fukamichi K 1981 *Phys. Lett.* **85A** 242–4
—— 1982 *J. Appl. Phys.* **53** 2226–8
Hiroyoshi H, Fukamichi K, Hoshi A and Nakagawa Y 1983 *High Field Magnetism* ed. M Date (Amsterdam: North-Holland) pp 113–6
Hiroyoshi H, Fukamichi K, Kikuchi M, Hoshi A and Masumoto T 1978 *Phys. Lett.* **65A** 163–5
Hiroyoshi H, Noguchi K, Fukamichi K and Nakagawa Y 1985 *J. Phys. Soc. Japan* **11** 3554–61
Kakehashi Y 1987 *J. Magn. Magn. Mater.* **66** L163–6
Kazama N S, Fujimori H and Watanabe H 1980 *J. Magn. Magn. Mater.* **15–18** 1423–4
Kubaschewski O 1982 *Iron–Binary Phase Diagrams* (Berlin: Springer-Verlag) pp 57–9
Matsuura M, Wakabayashi H, Goto T, Komatsu H and Fukamichi K 1989 *J. Phys.: Condens. Matter* **1** 2077–86
Palmar R G 1983 *Heidelberg Colloquium on Spin Glasses* ed. J L Van Hemmen and I Morgenstern (Berlin: Springer-Verlag) pp 234–51
Palstra T T M, Nieuwenhuys G J, Mydosh J A and Buschow K H 1985 *Phys. Rev.* B **31** 4622–32
Read D A, Moyo T and Hallam G C 1984 *J. Magn. Magn. Mater.* **44** 279–86
—— 1986 *J. Magn. Magn. Mater.* **54–57** 309–10
Ryan D H, Coey J M D, Batalla E, Altounian Z and Strom-Olsen J O 1987a *Phys. Rev.* B **35** 8630–8
Ryan D H, Coey J M D and Strom-Olsen J O 1987b *J. Magn. Magn. Mater.* **67** 148–54
Saito N, Hiroyoshi H, Fukamichi K and Nakagawa Y 1986 *J. Phys. F: Met. Phys.* **16** 911–9
Soukoulis C M, Levin K and Grest G S 1983 *Phys. Rev.* B **28** 1495–9
Takeda Y, Morimoto S, Ito A, Sato T and Miyako Y 1985 *J. Phys. Soc. Japan* **54** 2000–8
Unruh K M and Chien C L 1983 *J. Magn. Magn. Mater.* **31–34** 1587–8
Verbeek B H, Nieuwenhuys G J, Stocker H and Mydosh J A 1978 *Phys. Rev. Lett.* **40** 586–9
Wakabayashi H 1988 *PhD Thesis* Tokyo Institute of Technology
Wakabayashi H, Goto T, Fukamichi K, Komatsu H, Morimoto S and Ito A 1989 *J. Phys. Soc. Japan* **58** 3383–91
Xiao G and Chien C L 1987 *J. Appl. Phys.* **61** 3246–8